




ORIGINAL ARTICLE

Identification of regions maintaining atrial fibrillation through cycle length and cycle length gradient mapping

Masafumi Shimojo M.D.^{1,2} | Yasuya Inden M.D., Ph.D.²  | Satoshi Yanagisawa M.D., Ph.D.²  |
Ryota Yamauchi M.D.² | Kei Hiramatsu M.D.² | Tomoya Iwawaki M.D.² |
Masaya Tachi M.D.² | Shun Kondo M.D.² | Takayuki Goto M.D.² |
Yukiomi Tsuji M.D., Ph.D.^{1,2}  | Toyoaki Murohara M.D., Ph.D.²

¹Department of Cardiovascular Research and Innovation, Nagoya University Graduate School of Medicine, Nagoya, Japan

²Department of Cardiology, Nagoya University Graduate School of Medicine, Nagoya, Japan

Correspondence

Yasuya Inden, Department of Cardiology, Nagoya University Graduate School of Medicine, 65 Tsurumai-cho, Showa-ku, Nagoya, Aichi 466-8550, Japan.
Email: inden@med.nagoya-u.ac.jp

Abstract

Background: Visualizing the specific regions where atrial fibrillation (AF) is maintained is crucial for effective treatment, but it remains challenging in clinical practice. We aimed to address this challenge by developing a mapping approach focused on the cycle length (CL) and its gradient (CL-gradient).

Methods: In 105 patients undergoing initial ablation for persistent AF, pre-ablation CARTOFINDER data were utilized to create maps based on three indicators: (1) CL, the atrial frequency during AF calculated using CARTOFINDER; (2) Short CL, encompassing CLs within 5 ms of the minimum CL; and (3) CL-gradient, the CL range within a 6 mm radius. We evaluated the association between the AF termination through ablation and the measured values and patterns in each map.

Results: AF termination occurred in 17 patients. The AF termination group exhibited the significant large maximum CL-gradient (48.8 ms [interquartile range, 38.6–66.3], $p < .001$) and the short distance between the minimum CL site and the maximum CL-gradient site (15.8 mm, [interquartile range, 6.0–23.2], $p = .029$). Of the 17 AF termination cases, 13 exhibited a CL distribution pattern characterized by a steep CL-gradient near the minimum CL site (SG-MCL), defined as the distance of less than 23.2 mm and the maximum CL-gradient greater than 33.1 ms. In these AF termination cases, SG-MCL was also correlated with the ablation area.

Conclusions: The minimum CL area accompanied by significant CL gradients in the immediate vicinity may play a crucial role in sustaining AF.

KEYWORDS

atrial fibrillation, catheter ablation, cycle length, cycle length gradient, driver

This is an open access article under the terms of the [Creative Commons Attribution-NonCommercial-NoDerivs](https://creativecommons.org/licenses/by-nc-nd/4.0/) License, which permits use and distribution in any medium, provided the original work is properly cited, the use is non-commercial and no modifications or adaptations are made.

© 2024 The Author(s). *Journal of Arrhythmia* published by John Wiley & Sons Australia, Ltd on behalf of Japanese Heart Rhythm Society.

1 | INTRODUCTION

In general, circuit of organized arrhythmias can be mapped, and based on these visualized circuits, optimal treatment sites can be determined. However, mapping circuits in AF is challenging causing a reliance on empirical strategies. The inability to develop strategies based on individual AF mechanisms is a significant problem. Therefore, the visualization of AF mechanisms and development of individualized strategies based on the visualization can be a breakthrough for the treatment of AF.

In basic research, a rotor has been proposed as an area driving AF (AF driver), and its visualization has been conducted using a phase map.¹ Some studies have explored rotor visualization using a phase map in a clinical setting,²⁻⁴ but it is not possible to create a true phase map of a living human body. Evaluating the distribution of the atrial frequency is an alternative approach to mapping AF propagation.⁵⁻¹² During AF, the atrial frequency at a given point peaks at a certain value. Overall, it is known to have a hierarchical distribution throughout the atrium.^{7,8} Regions with high-frequency are considered to be upstream in fibrillatory conduction, and it is believed that AF drivers exist in these regions.

CARTOFINDER is equipped with a function that utilizes unipolar electrograms to calculate the atrial frequency during AF as the cycle length (CL). In this study, we used data obtained from clinical cases using CARTOFINDER. We focused on the distribution of CL and CL-gradient within the atrium and assessed the characteristics of regions presumed to be AF drivers.

2 | METHODS

2.1 | Study population

We performed a retrospective analysis of data collected from a catheter ablation database at the Nagoya University Hospital in Japan. This study was approved by our institutional ethics committee. We included consecutive 108 patients in this study who underwent initial radiofrequency catheter ablation for persistent AF performed at the Nagoya University Hospital between May 2020 and April 2023 and had whole left atrial CAROFINDER maps created before catheter ablation. The indications for catheter ablation for AF were based on the standardized guidelines.¹³ Written informed consent was obtained from all patients prior to the ablation procedure. The study was performed in accordance with the principles of the Declaration of Helsinki.

2.2 | Electrophysiology and mapping procedure

Details of electrophysiology and mapping procedure were described in the Supplemental Methods. A CARTOFINDER map of the left atrium was created before the ablation procedure by sequentially acquiring electrical signals using a mapping catheter. During this

recording process, the mapping catheter was left in place for at least 20 seconds at each location.

CARTOFINDER, developed to detect specific electrogram patterns during AF,¹⁴ also measures the CL at each recording site based on the annotations of unipolar electrograms. We utilized the data to conduct our own analysis. However, since it originally lacked the ability to display CL as a 3-dimensional (3-D) map, the patients in this study did not undergo an evaluation of CL distribution during the procedure.

2.3 | Catheter ablation

Details of ablation procedure have been previously described.¹⁵ The treatment strategy adopted for the patients in this study was as follows: Initially, pulmonary vein isolation (PVI) was performed during AF. If AF persisted after PVI, additional ablation such as left atrial posterior wall isolation (LAPWI) was performed at the operator's discretion. We did not perform ablation guided by CL as an indicator. If sinus rhythm was still not achieved, external cardioversion was conducted. In some cases, external cardioversion was performed with PVI alone. If AF converted to atrial tachycardia (AT) following ablation, ablation was performed for the AT. If frequent atrial ectopic beats were observed after restoration of sinus rhythm, ablation was considered for the ectopic beats. Following restoration of sinus rhythm, all cases underwent cavotricuspid isthmus line ablation, even if common atrial flutter had not been clinically documented.

2.4 | Evaluation of the reliability of FINDER-CL and selection of high-reliability samples

We assessed the reliability of FINDER-CL as an indicator of the atrial frequency. The detailed methods were described in the Supplemental Methods and illustrated in [Figure S1](#), [S2](#), and [S3](#). We assessed the stationarity of the CL by evaluating the temporal changes in annotation intervals. The reliability of FINDER-CL was examined by comparing it to the inverse of the dominant frequency (DF), obtained through the Fourier transformation of unipolar electrograms. To select reliable FINDER-CL samples, we conducted clustering on all the samples using the k-means method. These analyses were performed in a Python 3 (version 3.10.9) environment.

2.5 | The CL map, short CL map, and CL-gradient map

We utilized samples selected through the reliability assessment of FINDER-CL to reconfigure CL maps for each case, evaluating the distribution of CL within the left atrium ([Figure 1a](#)). We measured the values of the minimum CL, maximum CL, and CL range (the difference between maximum CL and minimum CL).

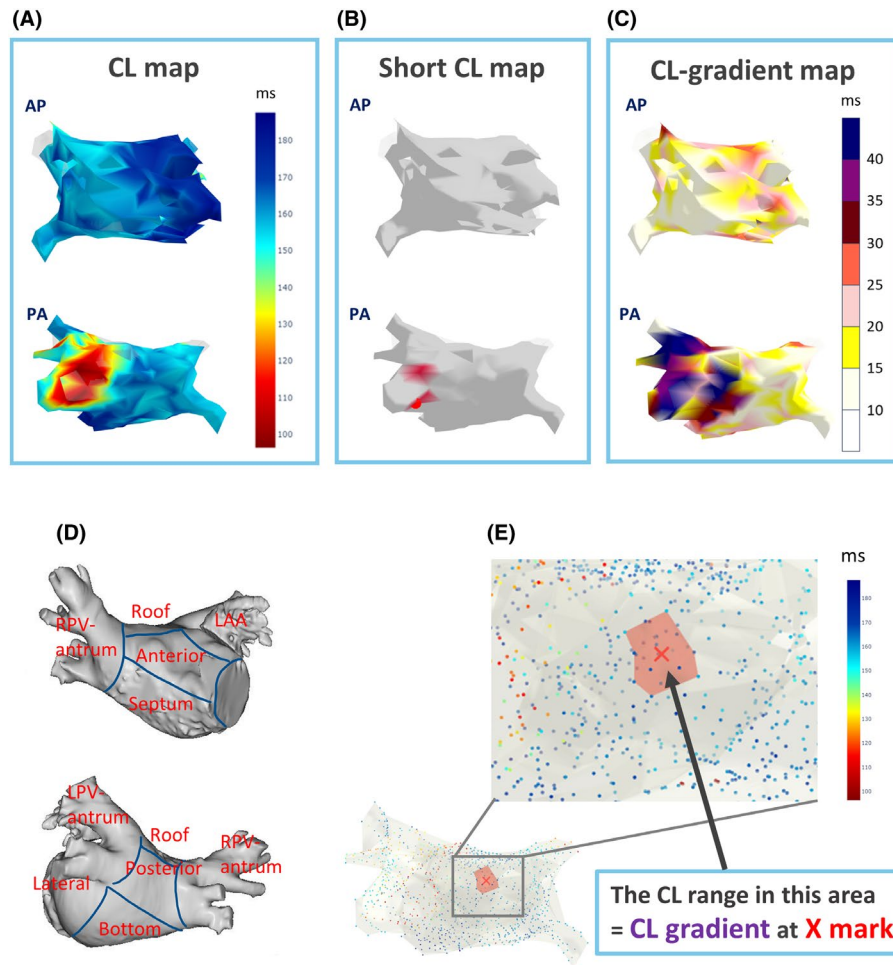


FIGURE 1 The concept of each map. (A) CL map: Colors represent CL; (B) Short CL map: Red areas show short CLs. The minimum CL is indicated by a red circle; (C) CL-gradient map: Colors represent CL-gradient; (D) Definition of areas within the left atrium; (E) CL-gradient concept: The color of the points represents the CL of each point. The CL-gradient at the X mark is defined as the CL range within a 6 mm radius centered on the X mark in the red area. CL, cycle length; RPV, right pulmonary vein; LPV, left pulmonary vein; LAA left atrial appendage.

To highlight areas with particularly short CL, we created a short CL map (Figure 1b). We defined short CL as values within 5 ms of the minimum CL (including the minimum CL). The areas where short CLs were recorded were evaluated based on the nine regions indicated in Figure 1d, along with the areas where the minimum CL was recorded. The cases were categorized as single type when short CLs were observed in the same area, and multiple type when they were observed across multiple areas.

We created a CL-gradient map to represent the strength of gradients occurring around each recording point (Figure 1c). The CL-gradient at a given point was calculated as the range of CL recorded within a 6 mm radius area from the point (Figure 1e). Detailed information about the CL-gradient map is shown in Supplemental Methods. We measured the values of the maximum CL-gradient, CL-gradient at the points of maximum CL and minimum CL, and the distance between the minimum CL site and the maximum CL-gradient site.

In order to examine the impact of the left atrial diameter (LAD) on CL range and CL-gradient, we investigated the correlation between the LAD and CL range, and the CL-gradient.¹⁶

2.6 | Definition and detection of AF driver

We hypothesized that if AF was terminated during ablation, there may be AF drivers at the ablation site where termination occurred.¹⁷ By focusing on these cases, it was possible to investigate the characteristics of the AF driver in clinical scenarios. Therefore, we assessed the distribution of CL and CL-gradient, and the correlation with AF termination. AF termination includes cases where AF directly converted to sinus rhythm and cases where AF transformed into AT.

The clinical course after ablation was followed up for more than 1 year.

2.7 | Statistical analysis

All statistical analyses were performed using R (version 4.0.3). Continuous variables were presented using mean and standard deviation or the median and interquartile range (IQR). For parametric tests, we conducted Student's *t*-test to compare the two groups. For

non-parametric tests, we used the Wilcoxon signed-rank test for comparing the two groups. Categorical variables were expressed in numbers and percentages. Fisher's exact test was used to compare categorical variables, and the Holm method was employed for the subsequent multiple testing. The augmented Dickey-Fuller test was used to assess stationarity in time series data, confirming its presence in cases of statistical significance. We calculated the Pearson correlation coefficient for binary correlations and plotted the approximate curve through simple linear regression analysis. The statistical significance was set at p -value <0.05 .

3 | RESULTS

3.1 | Assessment of reliability of FINDER-CL and sample selection

We assessed a total of 52,160 points obtained from 108 patients. Detailed results of the reliability assessment for FINDER-CL are provided in the Supplemental Results and [Figure S4](#), [S5](#), and [S6](#). As a result of the sample selection process, three out of 108 patients were excluded from the analysis because their 3-D CL maps only covered a part of the left atrium due to the lack of points. Consequently, we conducted a case analysis on 105 patients after excluding the three patients with fewer points.

3.2 | Study population

The baseline characteristics of 105 patients are summarized in [Table 1](#). The mean follow-up period was 12.6 ± 5.8 months. The mean AF duration from diagnosis was 2.5 ± 3.0 years, and the mean duration of persistent AF was 14.3 ± 19.3 months. The mean number of antiarrhythmic drugs was 1.1 ± 0.7 . AF termination was observed in 17 patients (16.2%), and AF recurrence was observed in 20 patients (19.0%). In 16 out of 17 patients in whom AF was terminated during the ablation, sinus rhythm was maintained within the observational period. Patients with AF termination compared to the non-termination group had smaller left atrial diameter (39.5 ± 7.4 mm vs. 44.4 ± 5.7 mm, $p = .002$), and patients with AF recurrence compared to the non-recurrence group had longer time from initial diagnosis (4.8 ± 5.0 years vs. 1.9 ± 2.1 years, $p < .001$).

The detailed ablation procedures are presented in [Table S1](#). PVI and cavotricuspid isthmus line ablation were performed in all patients, and LAPWI was performed in 57 patients (54.3%).

3.3 | CL map, short CL map and CL-gradient map

CL map measurements are illustrated in [Figure 2a](#). Patients with AF termination compared to the non-termination group had larger maximum CL (median 200.6 ms, IQR 187.6 to 223.1 vs 183.1 ms, IQR

TABLE 1 Baseline characteristics.

	All (n = 105)	AF termination		p-value	AF recurrence		p-value
		No (n = 88)	Yes (n = 17)		No (n = 85)	Yes (n = 20)	
Age, years old	63.6 \pm 10.3	63.1 \pm 10.3	66.0 \pm 10.3	.293	63.1 \pm 10.4	64.8 \pm 10.1	.561
Male	88 (83.8)	74 (84.1)	14 (82.4)	1.000	73 (85.9)	15 (75.0)	.309
Heart failure	25 (23.8)	18 (20.5)	7 (41.2)	.115	19 (22.4)	6 (30.0)	.560
Hypertension	63 (60.0)	55 (62.5)	8 (47.1)	.284	49 (57.6)	14 (70.0)	.447
Diabetes mellitus	13 (12.4)	10 (11.4)	3 (17.6)	.438	12 (14.1)	1 (5.0)	.454
Stroke	9 (8.6)	8 (9.1)	1 (5.9)	1.000	8 (9.4)	1 (5.0)	1.000
AF persistency, months	14.3 \pm 19.3	15.8 \pm 20.6	6.8 \pm 5.6	.078	12.6 \pm 16.4	21.5 \pm 28	.063
AF history, years	2.5 \pm 3.0	2.7 \pm 3.2	1.3 \pm 1.3	.087	1.9 \pm 2.1	4.8 \pm 5.0	<.001
Number of AADs	1.1 \pm 0.7	1.1 \pm 0.8	1.3 \pm 0.6	.266	1.1 \pm 0.7	1.2 \pm 1.0	.559
Class I AADs	6 (5.7)	5 (5.7)	1 (5.9)	1.000	4 (4.7)	2 (10.0)	.321
Beta blocker	62 (59.0)	49 (55.7)	13 (76.5)	.177	48 (56.5)	14 (70.0)	.319
Bepidil	41 (39.0)	35 (39.8)	6 (35.3)	.792	34 (40.0)	7 (35.0)	.801
Others	8 (7.6)	6 (6.8)	2 (11.8)	.613	7 (8.2)	1 (5.0)	1.000
eGFR, ml/min	63.1 \pm 15.3	64.1 \pm 15.0	57.9 \pm 16.1	.131	63.0 \pm 16.0	63.4 \pm 12.6	.901
BNP, pg/ml	104.2 (68.3–167.5)	102.7 (68.1–168.4)	106.7 (77.4–163.4)	.969	99.5 (68.3–163.4)	111.6 (76.1–191.6)	.503
LVEF, %	58.9 \pm 9.9	59.4 \pm 9.6	56.7 \pm 11.1	.313	59.0 \pm 10.6	58.5 \pm 5.8	.836
LAD, mm	43.6 \pm 6.2	44.4 \pm 5.7	39.5 \pm 7.4	.002	43.6 \pm 6.3	43.5 \pm 5.8	.903

Note: Values are given as a mean \pm standard deviation, n (%) or a median (interquartile range).

Abbreviations: AADs, anti-arrhythmic drugs; AF, atrial fibrillation; AF history, duration of atrial fibrillation history from diagnosis; BNP, brain natriuretic peptide; eGFR, estimated glomerular filtration rate; LAD, left atrial diameter; LVEF, left ventricular ejection fraction.

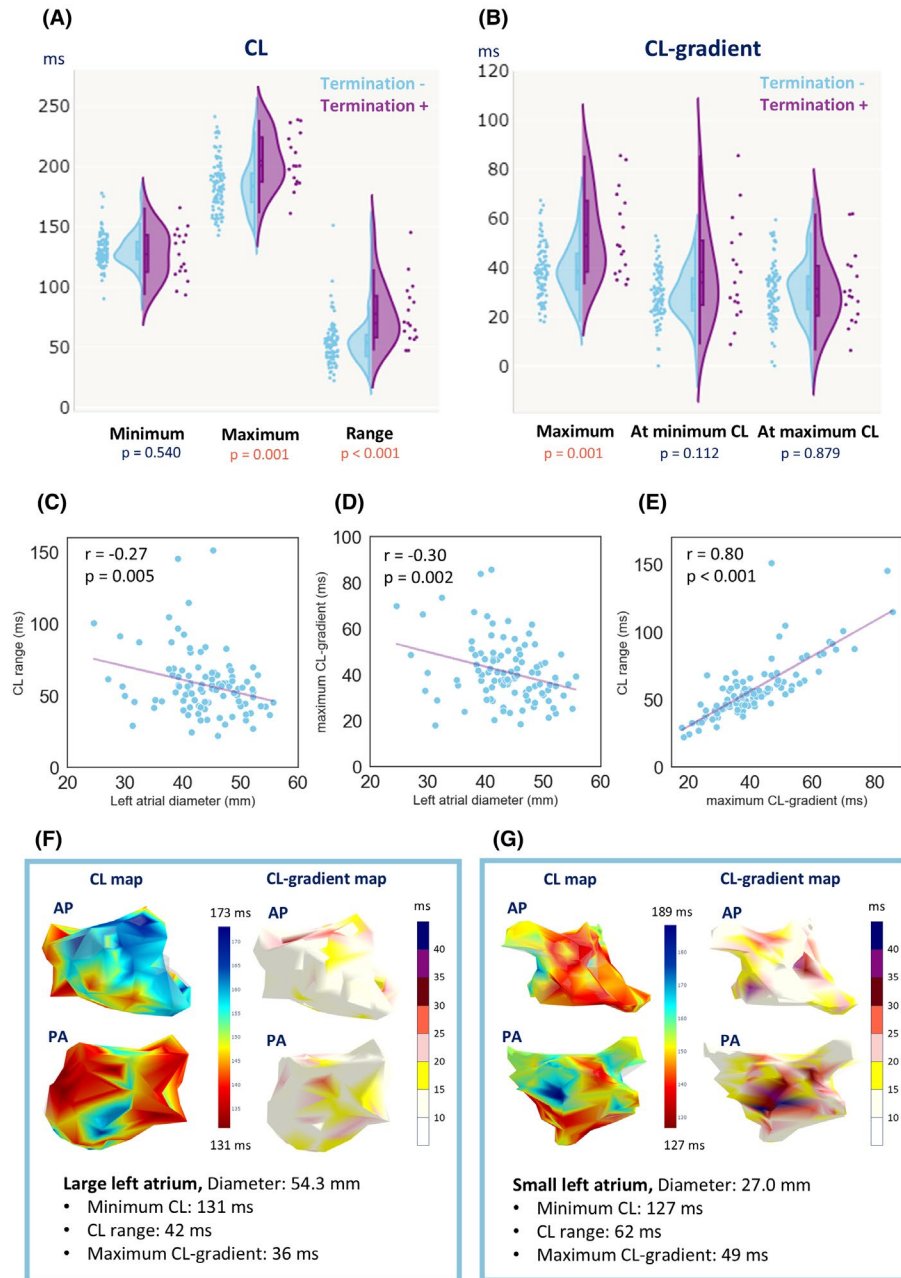


FIGURE 2 Violin plots illustrating results of CL and CL-gradient measurements. (A) CL measurements; (B) CL-gradient measurements. (C, D, E) The relationship among the CL-range, maximum CL-gradient, and the left atrial diameter. (F) an example of a large left atrium. (G) an example of a small left atrium. CL, cycle length; PA, posterior–anterior view; AP, anterior–posterior view.

170.4 to 194.2) and CL range (median 69.8 ms, IQR 58.4 to 91.3 vs 52.4 ms, IQR 42.6 to 60.1). No statistically significant difference was observed in the minimum CL between the groups.

The results of the CL-gradient setup are presented in the Supplemental Results and Figure S7. Results of the CL-gradient map are illustrated in Figure 2b. In patients with AF termination, the maximum CL-gradient (median 48.8 ms, IQR 38.6–66.3) was larger than those in non-termination patients (median 37.9 ms, IQR 31.2–45.5). No significant differences were observed in CL-gradient at the minimum CL site and the maximum CL site between the groups.

Figure 2c–g illustrates the correlations between the LAD and CL range, and the CL gradient. There was a negative correlation

between the LAD and CL range ($r = -0.27$, $p = 0.005$). Additionally, there was a negative correlation between the LAD and CL-gradient ($r = -0.30$, $p = 0.002$). Furthermore, CL-gradient showed a strong association with the CL range ($r = 0.80$, $p < 0.001$).

Figure 3 shows the distance between the minimum CL site and the maximum CL-gradient site. This distance was significantly shorter in AF termination group (median 15.8 mm, IQR 6.0–23.2) compared to the non-AF termination group (median 28.1 mm, IQR 12.6–47.3).

Comparison between the CL and CL-gradient measurements between the groups are shown in Table S2.

All cases are plotted according to two parameters associated with AF termination: maximum CL-gradient and the distance

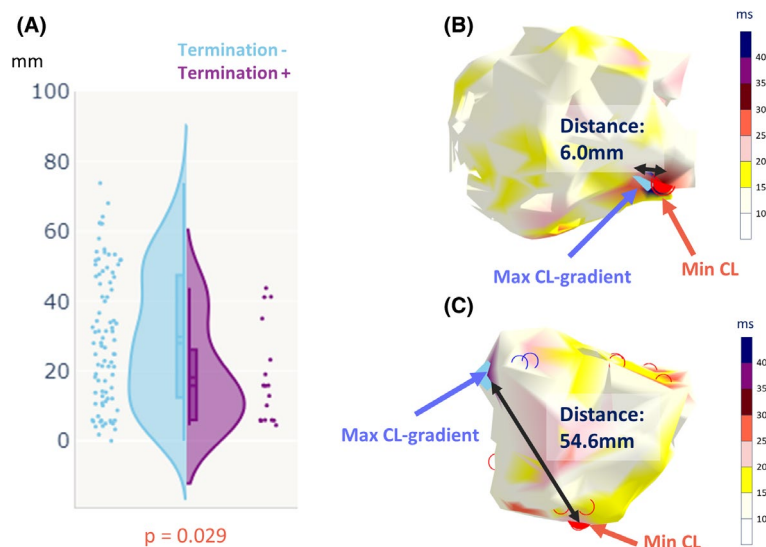


FIGURE 3 The minimum CL site and the maximum CL-gradient site (A) Violin plots illustrating the distance between the minimum CL site and the maximum CL-gradient site; (B) Example of a short distance case of AF termination; (C) Example of a long-distance case of AF termination. AF, atrial fibrillation; CL, cycle length.

between the minimum CL site and the maximum CL-gradient site. Each case is classified by whether AF terminated and whether the map pattern was single type or multiple type in the short CL map (Figures 4a and 5a). AF termination was frequently observed in cases where the distance between the minimum CL and the maximum CL-gradient was short (<23.2mm) and the maximum CL-gradient was large (>33.1ms). This area was designated as the pattern of steep gradient near the minimum CL (SG-MCL) (Figure 4a). Of the 17 AF termination cases, 13 showed SG-MCL, and of these 13 cases, 12 exhibited a single type. Additionally, among the 25 cases with pre-ablation map showing SG-MCL and a single type, AF terminated in 48.0% (12/25) of cases through PVI or LAPWI. Examples are provided to illustrate cases with and without SG-MCL (Figure 4b).

In Figure 5b, the minimum CL values are plotted for each region where the minimum CL was observed, with each case classified by whether AF terminated and whether the map pattern was single type or multiple type in the short CL map. When the minimum CL was observed in areas other than PVs or roof, there were no cases falling below 115ms. Conversely, when the minimum CL was observed in the PVs or roof, some cases showed relatively short CL. In these cases, a single type was more common, and AF termination was more frequently observed.

3.4 | Details of the AF termination group

Details of patients with AF termination are described in Table S3. In 11 patients, AF directly converted to sinus rhythm, and in six patients AF changed to AT. In 14 out of 17 patients (82.4%), there was a correlation between the isolation area leading to the AF termination and the area where the minimum CL was observed.

Figure 6a; Figure S8 illustrate cases of AF converting to sinus rhythm, with Figure 6a as a single type and Figure S8 as multiple type in the short CL map. Figure 6b and Figures S9 and S10 depict cases where AF converted to AT. In these cases, AF terminated by PVI or LAPWI. Notably, the minimum CL itself was not directly

ablated, and AF sometimes terminated before isolation was complete. Figure S11 shows cases where AF terminated by septal ablation. Although CL or CL-gradient were not used as ablation targets, the septal area exhibited short CLs with a steep CL-gradient. In most cases, CARTOFINDER maps and voltage maps could not identify AF drivers, and it seems difficult to predict whether AF converted to sinus rhythm or AT based on the pre-ablation maps.

4 | DISCUSSION

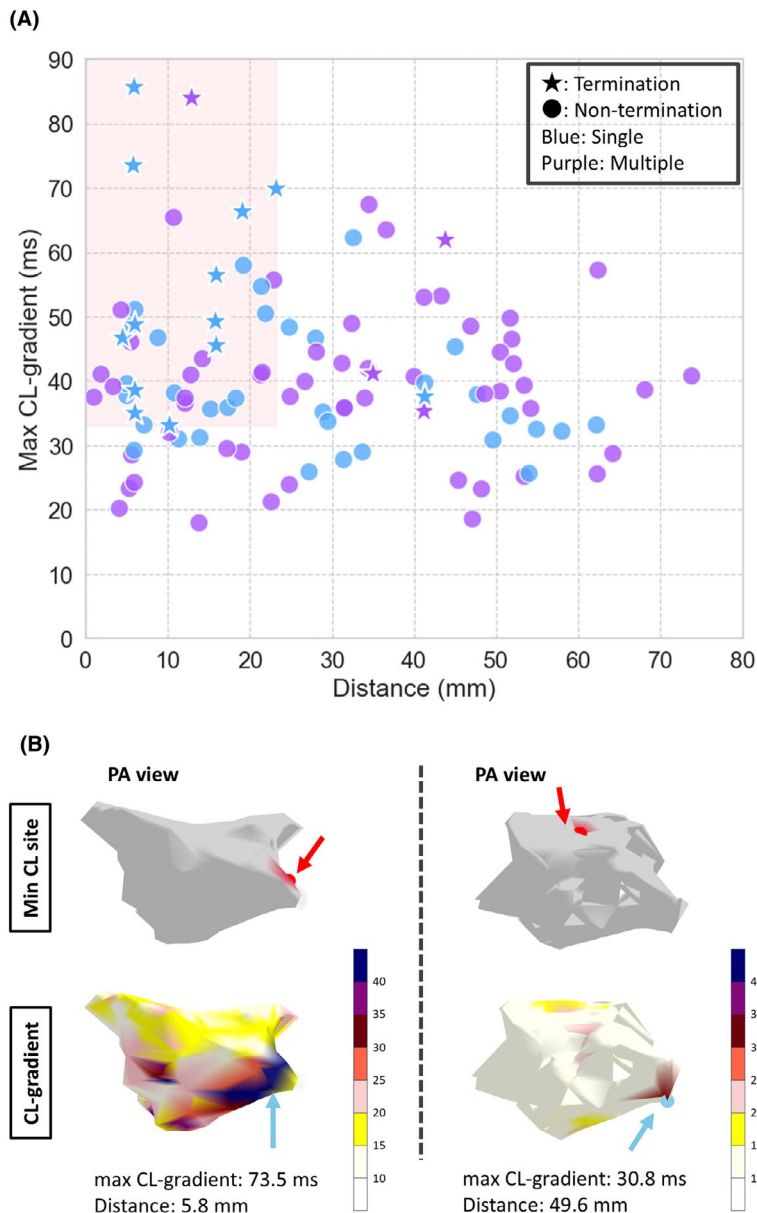
4.1 | Main findings

This study suggests that analyzing the distribution of CL and CL-gradient may help identify AF drivers and a minimum CL with a steep CL-gradient could be a potential AF driver. The novelty of this study lies in the adoption of higher-density mapping compared to previous studies,^{9,12} enabling a detailed evaluation of CL and CL-gradient distribution during AF in clinical cases.

4.2 | FINDER-CL as a means of atrial frequency analysis

CARTOFINDER employs a sequential mapping approach, requiring careful consideration of the validity when constructing maps from samples obtained at different timings during AF. In this study, 96.7% of all samples exhibited stationarity in CL. Additionally, as indicated by Figure S5b, the majority of the selected samples exhibited similar values with coefficients of variation around 0.2. From these results, it may be inferred that the CL observed at a certain point does not take completely random values, but it converges to a specific value with some degree of variability. It is well-documented that the AF signal invariably exhibits a peak upon the Fourier transformation,^{5,6} suggesting that atrial frequency might converge to a certain value during AF. Walters et al. have

FIGURE 4 Characteristics of CL-gradient. (A) The distance from the minimum CL to the maximum CL-gradient is plotted on the x-axis, and the maximum CL-gradient values are plotted on the y-axis for all cases. Stars: Cases where AF terminated; circles: Cases where AF did not terminate; blue: Cases classified as single in the short CL map; purple: Cases classified as multiple. The red background area indicates the pattern of steep gradient near the minimum CL (SG-MCL). (B) Short CL maps and CL-gradient maps. Left: A case of SG-MCL where AF terminated by right pulmonary vein isolation; right: A case of non-SG-MCL where AF did not terminate. AF, atrial fibrillation; CL, cycle length.



demonstrated the spatial-temporal stability of AF activation.¹⁸ Furthermore, the case illustrated in Figure S12 suggests the existence of cases where the CL distribution consistently follows a certain pattern. Therefore, we believe that using sequential mapping is justified for assessing atrial frequency.

In the frequency analysis of AF, DF has often been employed.⁵⁻¹² We demonstrated a strong correlation between FINDER-CL and DF (Figure S4), suggesting that FINDER-CL is a suitable indicator for atrial frequency.

4.3 | The pattern of steep CL-gradient near the minimum CL

The minimum CL values did not differ between the AF termination group and the non-termination group. This suggests that CL should not be evaluated as an absolute value, but rather assessed relatively

for each case. Additionally, the possible values of CL may depend on the histological properties of the location (Figure 5b). On the other hand, in the AF termination group, there were significantly larger values observed for the maximum CL, CL range and the maximum CL-gradient (Figure 2). The distance between the minimum CL site and the maximum CL-gradient site was closer in the AF termination group than in the AF non-termination group (Figure 3). We defined this feature as SG-MCL (Figure 4). Additionally, in the AF termination group, there was a correlation between the ablation region during AF termination and the region where SG-MCL was recorded (Figure 6; Table S3 and Figure S8-11).

Previous studies have suggested the presence of AF drivers in areas with the highest frequency.^{6-9,11,15} However, equally important is the fact that there is a significant CL-gradient in the vicinity. Kalifa et al., employing optical mapping experiments on sheep, demonstrated that the region around an AF driver exhibits the highest DF, with a pronounced decrease in DF in its immediate surroundings.¹¹

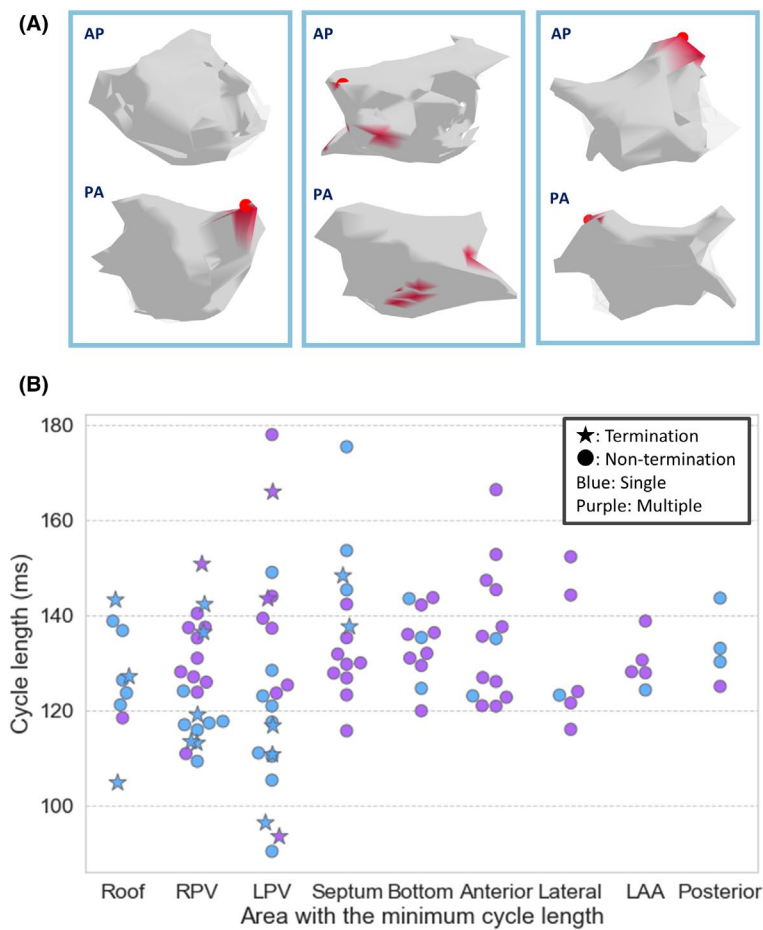


FIGURE 5 (A) Examples of short CL map. Left: Single type. Middle: Multiple type. Right: Single type. (B) Distribution of the minimum CL and characteristics of CL map. The minimum CL values for all cases are plotted for each area where the minimum CL was observed. Stars: Cases where AF terminated; circles: Cases where AF did not terminate; blue: Cases classified as single in the short CL map; purple: Cases classified as multiple. AF, atrial fibrillation; CL, cycle length; LAA, left atrial appendage; LPV, left pulmonary vein; RPV, right pulmonary vein.

One proposed mechanism for the formation of AF drivers is the electrical instability attributed to anatomical features. Anatomical factors such as abrupt changes in atrial fiber orientation or atrial wall thickness,^{19,20} contribute to conduction delays and blocks through mechanisms like source-sink mismatch,²¹ resulting in the dynamic AF propagation. The presence of SG-MCL in normal voltage regions and its detection sites supports this hypothesis (Figure 6). Furthermore, AF termination by ablating regions with steep gradients, even before the ablation of the minimum CL itself or the complete isolation of the minimum CL, suggests that AF drivers may represent a dynamic system involving both high and low-frequency components rather than merely an association with high-frequency domains.^{10,22,23}

4.4 | The distribution of CL and clinical implications

In this study, AF terminated in most cases by PVI or LAPWI, and the minimum CL was observed as a single type in the PVs or roof region (Figures 4 and 5), suggesting that AF termination may be limited to specific instances where AF was maintained by a single driver in the PVs or the LAPW. Although it is said that AF termination during ablation is not related to long-term outcomes, in this study, 16 out of 17 cases where AF terminated maintained sinus rhythm for over a year, suggesting that all AF drivers were effectively eliminated through PVI or LAPWI, which are reliable isolation methods.

While SG-MCL may be important as a component of a single AF driver, the CL distribution may become more complex due to interactions among drivers when multiple AF drivers are present. The case shown in Figure S8 suggests that drivers were present in both the LPV and RPV. This case exhibited a multiple pattern because their CLs were similar. In contrast, in the case shown in Figure S10, a repeated CL map was created after LAPWI, detecting a driver with a longer CL in a different location. However, identifying this driver from the initial CL distribution, which shows a single type, is challenging. Similarly, in the case that converted to AT (Figure 6b; Figure S9), detecting AT based on the initial CL distribution is difficult. Therefore, even if multiple drivers were present initially, if their CLs differed significantly, the CL distribution might be dominated by the driver with the shortest CL, resulting in a single type. This suggests the necessity of repeating the CL map after ablation.

We observed cases where the CL-gradient was low throughout the entire left atrium, and AF did not terminate in these cases. The maximum CL-gradient showed a negative correlation with LAD (Figure 2C–G), suggesting that cases with low CL-gradients are likely to have advanced structural remodeling of the left atrium. In such cases, AF may not be maintained by a single driver but could involve multiple drivers or a broad area, indicating a more complex maintenance mechanism.²⁴ Alternatively, if the minimum CL does not have steep CL-gradient, the minimum CL may have different meanings other than AF driver, such as an entrance for AF propagation from

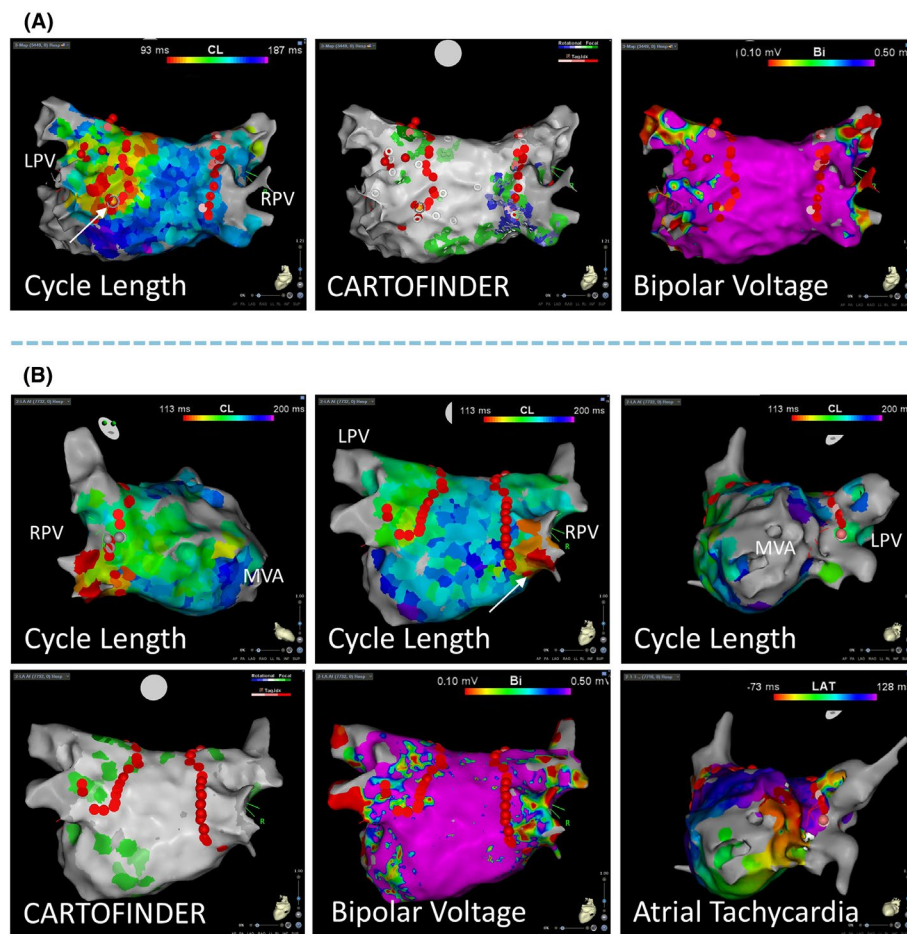


FIGURE 6 Case presentation. CL maps were revised based on the point selection conducted in this study. Red tags indicate ablation points. In CARTOFINDER maps, green denotes focal activities, and blue represents rotational activations. Voltage maps were created during AF. (A) PVI was started from the LPV. As ablation progressed downward from the roof of the posterior wall, AF converted to sinus rhythm when the bottom of the LPV was ablated (the white arrow). (B) After the LPV isolation was completed, AF converted to peri-mitral atrial tachycardia during ablation of the RPV bottom (the white arrow), despite the RPV isolation not being completed. AF, atrial fibrillation; CL, cycle length; LPV left pulmonary vein; PVI, pulmonary vein isolation; RPV right pulmonary vein.

the other driver chamber such as the epicardium, right atrium, and vein of Marshall.^{10,22,23}

4.5 | Study limitations

This study was a retrospective analysis conducted at a single center with a limited number of cases. Although there were no statistically significant differences in clinical outcomes based on the ablation strategy, the lack of uniformity in the strategies employed was a potential issue. The AF termination rate in the present study (16.2%) may be lower compared to other studies focusing on AF drivers.^{3,4,14} This could be attributed to several reasons, including the retrospective nature of the present study not being based on CL and not targeting AF termination as an endpoint, as well as the prevalence of cases with long-lasting persistent AF. Therefore, validation studies through prospective ablation strategies based on our findings are needed.

Although we have discussed the validity of the sequential mapping approach, it is worth highlighting that a whole-map analysis might be a preferable approach. However, if we use a whole-map approach, the mapping resolution may decrease,²⁴ leading to the distribution of the minimum CL and maximum CL-gradient, especially in narrow areas, to be overlooked. Additionally, the appropriate setting for the CL-gradient we proposed may depend on the density of the maps. An ideal mapping method would be both high-density and able to cover the entire region.

Our evaluation was based on the data from FINDER-CL. While we assessed the reliability of FINDER-CL and conducted the study by selecting samples with high reliability, there is a need for the development of more accurate software to calculate atrial frequencies. It is also important to note that FINDER-CL is based on unipolar electrograms, which may lead to potential accuracy degradation due to far-field potentials or low voltages.²⁵

We have only mapped the left atrium, but ideally, mapping should cover all chambers.^{10,22,23,26} With reports of drivers

observed in the right atrium,^{22,26} mapping of the right atrium could potentially improve the detection rate of drivers. However, encompassing all chambers includes not only the right atrium but also the epicardial side, Marshall vein, intraseptal areas, and coronary sinus. Mapping of all the regions in clinical cases is not practical.

5 | CONCLUSIONS

Mapping the CL and CL-gradient during AF can provide insights into the mechanisms of AF. This information may be valuable for guiding AF treatment.

ACKNOWLEDGMENTS

None.

FUNDING INFORMATION

N/A.

CONFLICT OF INTEREST STATEMENT

Drs. Shimojo and Tsuji are affiliated with a department sponsored by Japan Lifeline Co., Ltd, BIOTRONIK Japan, Inc., FUKUDA DENSHI Co., Ltd, and SUZUKEN Co., Ltd. Other authors have no conflict of interest.

DATA AVAILABILITY STATEMENT

The datasets generated and/or analyzed during the current study are available from the corresponding author on reasonable request.

ETHICS STATEMENT

This study was approved by ethics committee of Nagoya University. Written informed consent was obtained from all patients. The study was performed in accordance with the principles of the Declaration of Helsinki.

ORCID

Yasuya Inden  <https://orcid.org/0000-0001-5732-5672>

Satoshi Yanagisawa  <https://orcid.org/0000-0002-0658-5498>

Yukiomi Tsuji  <https://orcid.org/0000-0003-4836-3057>

REFERENCES

- Nattel S, Xiong F, Aguilar M. Demystifying rotors and their place in clinical translation of atrial fibrillation mechanisms. *Nat Rev Cardiol*. 2017;14(9):509–20.
- Sakata K, Okuyama Y, Ozawa T, Haraguchi R, Nakazawa K, Tsuchiya T, et al. Not all rotors, effective ablation targets for nonparoxysmal atrial fibrillation, are included in areas suggested by conventional indirect indicators of atrial fibrillation drivers: ExTRa mapping project. *J Arrhythm*. 2018;34(2):176–84.
- Narayan SM, Krummen DE, Shivkumar K, Clopton P, Rappel WJ, Miller JM. Treatment of atrial fibrillation by the ablation of localized sources: CONFIRM (conventional ablation for atrial fibrillation with or without focal impulse and rotor modulation) trial. *J Am Coll Cardiol*. 2012;60(7):628–36.
- Haissaguerre M, Hocini M, Denis A, Shah AJ, Komatsu Y, Yamashita S, et al. Driver domains in persistent atrial fibrillation. *Circulation*. 2014;130(7):530–8.
- Skanes AC, Mandapati R, Berenfeld O, Davidenko JM, Jalife J. Spatiotemporal periodicity during atrial fibrillation in the isolated sheep heart. *Circulation*. 1998;98(12):1236–48.
- Mandapati R, Skanes A, Chen J, Berenfeld O, Jalife J. Stable microreentrant sources as a mechanism of atrial fibrillation in the isolated sheep heart. *Circulation*. 2000;101(2):194–9.
- Mansour M, Mandapati R, Berenfeld O, Chen J, Samie FH, Jalife J. Left-to-right gradient of atrial frequencies during acute atrial fibrillation in the isolated sheep heart. *Circulation*. 2001;103(21):2631–6.
- Lazar S, Dixit S, Marchlinski FE, Callans DJ, Gerstenfeld EP. Presence of left-to-right atrial frequency gradient in paroxysmal but not persistent atrial fibrillation in humans. *Circulation*. 2004;110(20):3181–6.
- Sanders P, Berenfeld O, Hocini M, Jais P, Vaidyanathan R, Hsu LF, et al. Spectral analysis identifies sites of high-frequency activity maintaining atrial fibrillation in humans. *Circulation*. 2005;112(6):789–97.
- Wu TJ, Ong JJ, Chang CM, Doshi RN, Yashima M, Huang HL et al. Pulmonary veins and ligament of Marshall as sources of rapid activations in a canine model of sustained atrial fibrillation. *Circulation*. 2001;103(8):1157–63.
- Kalifa J, Tanaka K, Zaitsev AV, Warren M, Vaidyanathan R, Auerbach D et al. Mechanisms of wave fractionation at boundaries of high-frequency excitation in the posterior left atrium of the isolated sheep heart during atrial fibrillation. *Circulation*. 2006;113(5):626–33.
- Atienza F, Almendral J, Jalife J, Zlochiver S, Ploutz-Snyder R, Torrecilla EG, et al. Real-time dominant frequency mapping and ablation of dominant frequency sites in atrial fibrillation with left-to-right frequency gradients predicts long-term maintenance of sinus rhythm. *Heart Rhythm*. 2009;6(1):33–40.
- Nogami A, Kurita T, Abe H, Ando K, Ishikawa T, Imai K, et al. JCS/JHRS 2019 guideline on non-pharmacotherapy of cardiac arrhythmias. *J Arrhythm*. 2021;37(4):709–870.
- Honarbakhsh S, Schilling RJ, Dhillon G, Ullah W, Keating E, Providencia R, et al. A novel mapping system for panoramic mapping of the left atrium: application to detect and characterize localized sources maintaining atrial fibrillation. *JACC Clin Electrophysiol*. 2018;4(1):124–34.
- Shimojo M, Inden Y, Yanagisawa S, Riku S, Suga K, Furui K, et al. Identification of high priority focal activations in persistent atrial fibrillation using a novel mapping strategy. *Heart Vessel*. 2022;37(5):840–53.
- Njoku A, Kannabhiran M, Arora R, Reddy P, Gopinathannair R, Lakkireddy D, et al. Left atrial volume predicts atrial fibrillation recurrence after radiofrequency ablation: a meta-analysis. *Europace*. 2018;20(1):33–42.
- Zaman JAB, Sauer WH, Alhousseini MI, Baykaner T, Borne RT, Kowalewski CAB, et al. Identification and characterization of sites where persistent atrial fibrillation is terminated by localized ablation. *Circ Arrhythm Electrophysiol*. 2018;11(1):e005258.
- Walters TE, Lee G, Morris G, Spence S, Larobina M, Atkinson V, et al. Temporal stability of rotors and atrial activation patterns in persistent human atrial fibrillation: a high-density epicardial mapping study of prolonged recordings. *JACC Clin Electrophysiol*. 2015;1(1–2):14–24.
- Zhao J, Hansen BJ, Wang Y, Csepe TA, Sul LV, Tang A, et al. Three-dimensional integrated functional, structural, and computational mapping to define the structural "fingerprints" of heart-specific

- atrial fibrillation drivers in human heart ex vivo. *J Am Heart Assoc.* 2017;6(8):e005922.
20. Hansen BJ, Zhao J, Csepe TA, Moore BT, Li N, Jayne LA, et al. Atrial fibrillation driven by micro-anatomic intramural re-entry revealed by simultaneous sub-epicardial and sub-endocardial optical mapping in explanted human hearts. *Eur Heart J.* 2015;36(35):2390–401.
 21. Klos M, Calvo D, Yamazaki M, Zlochiver S, Mironov S, Cabrera JA, et al. Atrial septopulmonary bundle of the posterior left atrium provides a substrate for atrial fibrillation initiation in a model of vagally mediated pulmonary vein tachycardia of the structurally normal heart. *Circ Arrhythm Electrophysiol.* 2008;1(3):175–83.
 22. Hiram R, Naud P, Xiong F, aldatt D, Algalarrondo V, Sirois MG, et al. Right atrial mechanisms of atrial fibrillation in a rat model of right heart disease. *J Am Coll Cardiol.* 2019;74(10):1332–47.
 23. Jiang R, Buch E, Gima J, Upadhyay GA, Nayak HM, Beaser AD, et al. Feasibility of percutaneous epicardial mapping and ablation for refractory atrial fibrillation: insights into substrate and lesion transmural. *Heart Rhythm.* 2019;16(8):1151–9.
 24. Quintanilla JG, Shpun S, Jalife J, Filgueiras-Rama D. Novel approaches to mechanism-based atrial fibrillation ablation. *Cardiovasc Res.* 2021;117(7):1662–81.
 25. de Groot NMS, Shah D, Boyle PM, Anter E, Clifford GD, Deisenhofer I, et al. Critical appraisal of technologies to assess electrical activity during atrial fibrillation: a position paper from the European heart rhythm association and European Society of Cardiology Working Group on eCardiology in collaboration with the Heart Rhythm Society, Asia Pacific Heart Rhythm Society, Latin American Heart Rhythm Society and computing in cardiology. *Europace.* 2022;24(2):313–30.
 26. Lim HS, Hocini M, Dubois R, Denis A, Derval N, Zellerhoff S, et al. Complexity and distribution of drivers in relation to duration of persistent atrial fibrillation. *J Am Coll Cardiol.* 2017;69(10):1257–69.

SUPPORTING INFORMATION

Additional supporting information can be found online in the Supporting Information section at the end of this article.

How to cite this article: Shimojo M, Inden Y, Yanagisawa S, Yamauchi R, Hiramatsu K, Iwawaki T, et al. Identification of regions maintaining atrial fibrillation through cycle length and cycle length gradient mapping. *J Arrhythmia.* 2024;40:1389–1399. <https://doi.org/10.1002/joa3.13151>